PCCP

Dependence of Hot Electron Transfer on Surface Coverage and Adsorbate Species at Semiconductor-Molecule Interfaces

Journal:	*Physical Chemistry Chemical Physics*
Manuscript ID	CP-ART-10-2017-007247.R1
Article Type:	Paper
Date Submitted by the Author:	09-Apr-2018
Complete List of Authors:	Li, Lesheng; University of North Carolina at Chapel Hill, Chemistry Kanai, Yosuke; University of North Carolina at Chapel Hill, Department of Chemistry

Journal Name

ARTICLE

Dependence of Hot Electron Transfer on Surface Coverage and Adsorbate Species at Semiconductor-Molecule Interfaces

Received 00th January 20xx,
Accepted 00th January 20xx

DOI: 10.1039/x0xx00000x

www.rsc.org/

Lesheng Li and Yosuke Kanai*

Developing a molecular-level understanding of how hot electron transfer process can be enhanced at semiconductor-molecule interfaces is central to advancing various future technologies. Using first-principles quantum dynamics simulations, we investigate how surface coverage and molecular adsorbate species influence the hot electron transfer at semiconductor-molecule interfaces. Counterintuitively, hot electron transfer from semiconductor to molecules was found to be lessened with increased surface coverage because inter-molecular interaction changes nonadiabatic couplings across the semiconductor and adsorbed molecules. The adsorbate molecular species itself was found to be an important factor in hot electron transfer not simply because of the energy level alignments at the interface, but also because the transfer is quite sensitive to nonadiabatic couplings. Our work shows that relatively minor variations of the couplings could lead to significant changes in hot electron transfer characteristics at semiconductor-molecule interfaces. Controlling nonadiabatic couplings must be part of developing a molecular-level "design principle" for enhancing hot electron transfer in addition to the well-recognized importance of energy level alignments.

Introduction

Novel concepts based on hot charge carriers have attracted great attention in recent years for various technological applications, ranging from photodetector,[1-4] photovoltaic (PV),[5-7] to photocatalysis.[8] In these applications, hot electron transfer (HET) at heterojunctions between different materials plays a central role in their performance. For instance, hot carriers need to be extracted through selective energy contacts before thermalization takes over in so-called hot carrier solar cells.[9,10] HET from the semiconductor material to adsorbed molecule is also of great concern in PV and photoelectrochemical (PEC) devices that are based on dye-sensitized solar cells (DSSCs) concept[11-13] since such charge transfer process negatively impacts the device performance.[14-17]

Because understanding the HET process at a molecular level is central to realizing these novel applications, considerable efforts have been dedicated to investigating HET at various heterogeneous interfaces, such as quantum dot (QD) core-shell,[18] semiconductor-QDs,[19-21] semiconductor-metal,[22-26] and semiconductor-molecule.[27-29] Ultimately, one hopes to build a "design principle" at the molecular level for enabling and controlling HET for various applications. In spite of great advances made in this field,[17,27,30-35] developing a better understanding of HET[36,37] is complicated by having complex interplays among various dynamical processes excited electrons can go through[14,17]. In our recent first-principles quantum dynamics study of excited electron at semiconductor-molecule interface, the HET process from semiconductor to adsorbed molecule was observed.[29] This provided us with an atomistic model for studying how the HET can be tuned at the molecular level. In this work, we focus on understanding dependence of the HET on surface coverage and adsorbed molecular species at semiconductor-molecule interface by considering two widely-used dye molecules, Cyanidin and Alizarin. In particular, we discuss results of first-principles simulations for elucidating the impact of inter-molecular interaction and molecular electronic structure on the HET process.

Computational Details

Our calculations were performed using a computational approach[29,38] that combines first-principles molecular dynamics (FPMD) simulation and the single-particle fewest-switches surface hopping (FSSH) algorithm.[15,39-41] The detailed procedure has been discussed in our earlier works.[29,38] In order to obtain a better description of the energy level alignments at the heterogeneous interface, many-body perturbation theory calculations at the "one-shot" G_0W_0 level[42-44] were used to correct the Kohn-Sham (KS) eigenvalues from DFT calculations to obtain quasi-particle (QP) energies.

Department of Chemistry, University of North Carolina at Chapel Hill, Chapel Hill, North Carolina 27599, United States of America. Email: ykanai@unc.edu

† Electronic Supplementary Information (ESI) available: details of the interface models, peak probability of hot electron within unoccupied electronic states and hot electron accepting molecular states, surface-induced delocalization of the hot electron state for Cyanidin, nonadiabatic coupling, probability change for hot electron state before and after shifting energy level. See DOI: 10.1039/x0xx00000x

The FPMD simulations were performed for a duration of 2 ps with a time step of 0.48 fs at 295 K using a modified version of the Qbox code.[45] The KS wave functions were represented in a plane-wave basis using norm-conserving pseudopotentials[46] with energy cutoff of 50 Rydberg. The generalized gradient approximation by Perdew, Burke, and Ernzerhof (PBE)[47] was used for the exchange-correlation functional. The KS single-particle energies and nonadiabatic couplings (NACs, which are also referred to as vibronic couplings in literature) were obtained on-the-fly in the FPMD simulation. NAC describes how well electronic states are coupled by the lattice/ion motion, and the NAC matrix is numerically calculated according to the prescription by Hammes-Schiffer and Tully[40], as

$$D_{ij} = \langle \psi_i(R(t)) | \nabla_R | \psi_j(R(t)) \rangle \cdot \frac{dR}{dt}$$

$$= \left\langle \psi_i(R(t)) \left| \frac{\partial}{\partial t} \right| \psi_j(R(t)) \right\rangle$$

$$= \frac{\langle \psi_i(R(t)) | \nabla_R \hat{H} | \psi_j(R(t)) \rangle}{\varepsilon_j(R(t)) - \varepsilon_i(R(t))} \cdot dR/dt$$

where D_{ij} is the nonadiabatic coupling between two state i and j, $\psi_i(R(t))$ and $\varepsilon_i(R(t))$ are the single-particle eigenfunction and eigenvalue for state i at the nuclear coordinate $R(t)$, and $\hat{H}$ is the Kohn-Sham Hamiltonian. The time derivative is calculated in FPMD simulation by enforcing the phase continuity as in ref 48.

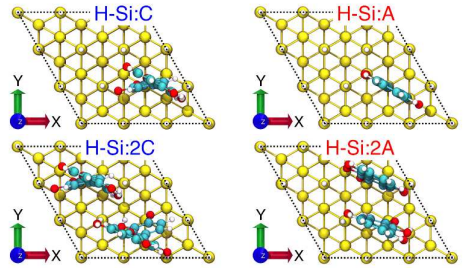

Figure 1. Top view of the simulation cells for the **H-Si:C**, **H-Si:2C**, **H-Si:A**, and **H-Si:2A** interfaces. The H-Si(111) surface was modeled using a 144-Si-atom slab with eight layers.

Quasi-particle (QP) energies were obtained by calculating many-body corrections to the KS eigenvalues within the "one-shot" G_0W_0 approximation,[42-44] starting from the KS wave functions and eigenvalues. The calculations employed the random-phase approximation for the screened Coulomb interaction, and the Godby-Needs plasmon-pole model[49,50] was used in calculating the dielectric function. The G_0W_0 calculations were performed at the equilibrium geometry using the Yambo code,[51] with the KS wave functions obtained from the Quantum Espresso code.[52] The convergence tests for the G_0W_0 calculations were performed as in our previous work.[29] The FSSH simulation[15,39-41] was performed in the single-particle description using the QP energies from the G_0W_0 calculation and the NACs from the FPMD simulation. The FSSH simulations were performed within the classical-path

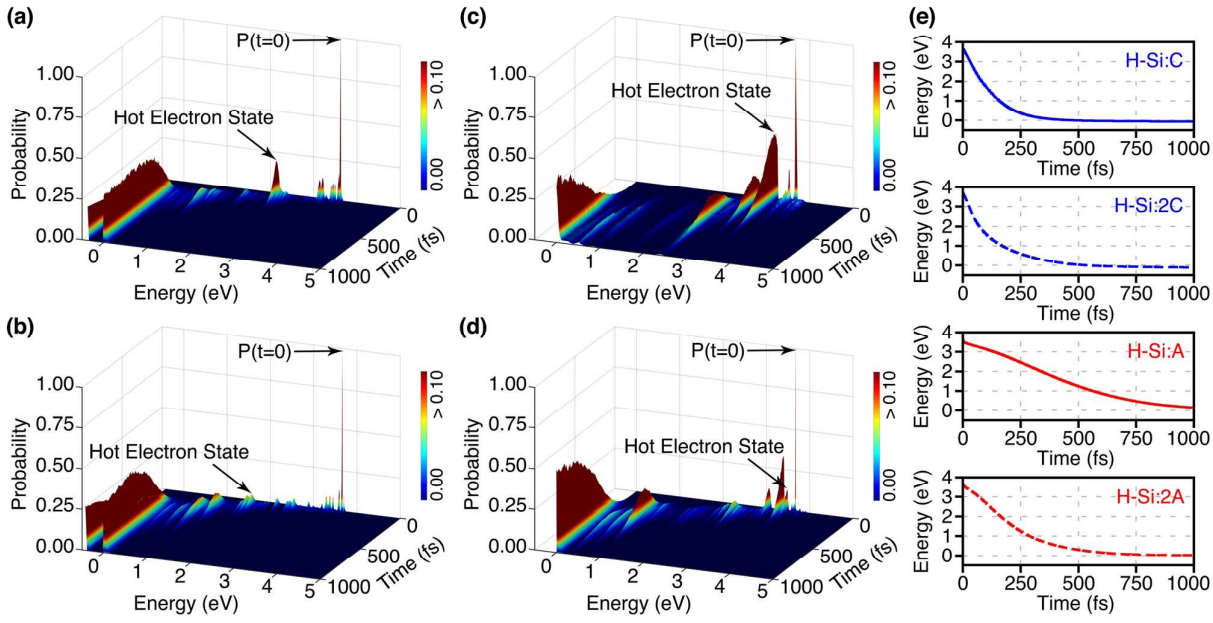

Figure 2. Probability of locating the excited electron at a specific energy as a function of time at the interfaces of (a) **H-Si:C**, (b) **H-Si:2C**, (c) **H-Si:A**, and (d) **H-Si:2A**, together with the (e) ensemble averaged energy for the excited electron. The reference energy of 0 eV corresponds to the surface CBM. The hot electron accepting state that dominantly localized on the molecule is referred to as hot electron state. The excited electron was initially populated in a semiconductor state with energy of ~3.6 eV above the surface CBM and is indicated by P(t=0). We also provide the figure (e) using the log scale in Supporting Information so that deviation from exponential behaviour is obvious.

approximation (CPA) as described in ref 29. This allows us to use a large number of atomic trajectories for converging the ensemble-averaged quantities because the trajectories do not depend on the hops when the CPA is adapted. First, an ensemble of 2116 trajectories was generated by taking a 1 ps trajectory from various different temporal points in the FPMD simulation. Each of these 1 ps long trajectories starts with different positions and momenta for atoms. Then, 500 FSSH simulations were performed for each trajectory, converging the sampling of the hopping probability distribution using the Monte Carlo method.

It is useful to comment on this first-principles simulation approach, contrasting to the recent first-principles Boltzmann Transport Equation (BTE) approach which describes the flow of collective electrons and phonons in phase space.[53] These two approaches are designed to describe the carrier dynamics in different limits of charge carrier density, and therefore their appropriateness depends on the context in which these approaches are employed. The present approach based on FSSH method provides the time-dependent statistical description of a single excited electron for an ensemble of the system (i.e. many interfaces with a single excited electron), and it is suitable when coupling of the excited electron dynamics to the lattice movement (i.e. ions) is the dominant factor in controlling the relaxation of the excited electron. In such a situation, the time-dependence of the probabilistic distribution can be modelled by performing FSSH stochastic simulation runs, and the algorithm is designed to satisfy the detailed balance for the ensemble.[15] There exist many reviews on the surface hopping approach, and ref 54-56 are, for example, useful for gaining perspectives on its strengths and limitations in general. Specific to our FSSH simulation in the single-particle framework, carrier-carrier scattering is not present unlike in the BTE approach. In the first-principles BTE approach, on the other hand, statistical behaviour of a collection of carriers is modelled by propagating probability density function in time. Bernardi and co-workers made significant advances with the first-principles BTE approach in recent years.[53,57-59] They have demonstrated how interaction between different quasi-particles (electrons, phonons, etc) can be obtained from first-principles calculations in the context of the many-body perturbation theory, and these properties are used to employ the semi-classical BTE for studying carrier dynamics in real materials. More rigorous approaches based on non-equilibrium Green's functions such as Kadanoff-Baym equation are also emerging in the context of first-principles approach in recent years. A comprehensive review can be found in ref 60.

Results and discussion

Representative semiconductor-molecule interfaces between a hydrogen-terminated Si(111) surface and two widely-used dye molecules, Cyanidin and Alizarin, were studied in this work to elucidate the impact of molecular electronic structure on the HET process. Our earlier work showed noticeable HET with Cyanidin adsorbed at the H-Si(111) surface.[29] Alizarin is one of the most widely studied dye molecules both experimentally and theoretically in the literature[30,61,62] partly because it has its unoccupied electronic states quite high energetically, often well above the conduction band minimum (CBM) of many semiconductors (see e.g. Figure S2 in the Supporting Information).[30] When studying semiconductor-molecule interfaces, the surface coverage could be another important factor. One might expect an enhanced HET simply because increased coverage increases the number of molecular states that can accept the hot electron from the semiconductor. At the same time, interactions among the adsorbed molecules could change the nature of those accepting molecular states. In order to examine how inter-molecular interaction influences the HET process, surface coverages of ~11% (in terms of the number of Si-H units at the surface) and ~22% were studied, as shown in Figure 1. The molecules are adsorbed and oriented such that the π-π interaction is maximized. There are essentially no inter-molecular interactions for the 11% coverage, but the adsorbed molecules are closely packed in the case of the 22% coverage and significant inter-molecular interactions exist. Short-hand notations are used for referring to the interface models as **H-Si:C** (11% coverage of Cyanidin), **H-Si:2C** (22% coverage of Cyanidin), **H-Si:A** (11% coverage of Alizarin), and **H-Si:2A** (22% coverage of Alizarin). Details of the interface models can be found in the Supporting Information.

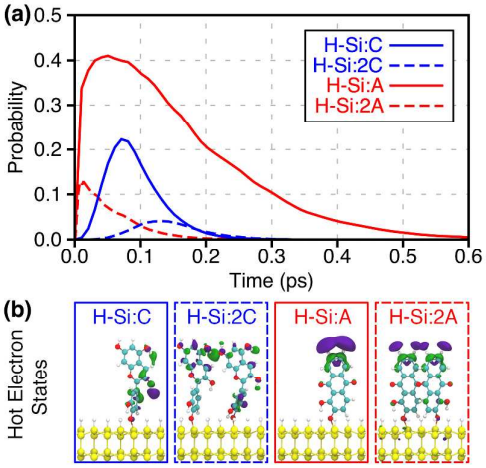

Figure 3. (a) Probability change and (b) isosurface of the single-particle Kohn-Sham electronic wave function of the hot electron states at the interfaces. Hot electron states become delocalized over both molecules when the surface coverage is increased.

Figure 2a-d shows the probability of locating the hot electron at a specific energy as a function of time for an ensemble of interfaces simulated at room temperature. The reference energy of 0 eV corresponds to the CBM of the semiconductor surface. For simulating dynamics of the hot electron, a highly-excited electron was initially placed in a semiconductor state with the energy of ~3.6 eV above the surface CBM. As can be seen in Figure 2a-d, the excited electron dynamics does not exhibit a simple monotonic decay for the probability change for any of these interfaces. In

particular, the **H-Si:A** interface (Figure 2c) yields very slow relaxation due to significant trapping of the hot electron within the adsorbed molecule before it relaxes down to the surface CBM. This HET into a localized state of the adsorbed molecule was observed most prominently for the **H-Si:A** interface, but to a lesser extent for all other interfaces. The molecular states that predominantly accept the hot electron are referred to as hot electron states throughout this paper. The hot electron state is located energetically at 1.34, 2.09, 0.40, and 0.18 eV below the initial excited electronic state at the **H-Si:C**, **H-Si:2C**, **H-Si:A**, and **H-Si:2A** interfaces, respectively (see Figure 2a-d). Time evolution of the ensemble-averaged energy for the hot electron is shown in Figure 2e, and they do not follow an exponential decay as observed at the clean H-Si(111) surface[29] because of the HET to the adsorbed molecules.

Peak probability and lifetime of the hot electron within the adsorbed molecule are the two key quantities of interest for characterizing the HET because they indicate the extent to which the hot electron transfers into the adsorbate and the extended time that the hot electron resides within the molecule. Probability changes for the hot electron states are shown in Figure 3a. As can be seen, the peak probability in the hot electron state is much greater for the low-coverage cases (**H-Si:C** vs. **H-Si:2C)** than for the high-coverage cases (**H-Si:A** vs. **H-Si:2A**), and it reaches as high as 0.42 for the **H-Si:A** interface (see Table 1). In addition to the peak probability, the residence time of the hot electron within the adsorbed molecule is another important factor for utilizing highly-excited electrons for some technological applications. We determined the hot electron lifetime in the molecule by calculating the full width at half maximum of the probability rise, and the results are summarized in Table 1. Although the **H-Si:2C** interface exhibits a longer residence time compared to the **H-Si:C** interface, the likelihood of finding the hot electron is very small. The hot electron lifetime within the adsorbed Alizarin molecule at the **H-Si:A** interface was found to be noticeably longer, comparable to the typical hot electron relaxation time for the clean H-Si(111) surface and bulk silicon.[29,63-68] At the same time, this lifetime is still much shorter than the typical time scales of redox reactions by adsorbed molecules at semiconductor-molecule interfaces, ranging from nanoseconds to microseconds.[69] We note also here that we do not observe excited electron relaxation *within* the molecule after the hot electron transfers into the molecule even though there exist other energetically-lower electronic states localized on the molecule. Rather, the hot electron transfers back to the semiconductor. Detail analysis can be found in the Supporting Information.

Table 1. Peak probability and residence time of hot electron within the adsorbed molecule at the interfaces.

Interface	H-Si:C	H-Si:2C	H-Si:A	H-Si:2A
Peak Probability	0.23	0.04	0.42	0.13
Residence Time (fs)	81	106	192	53

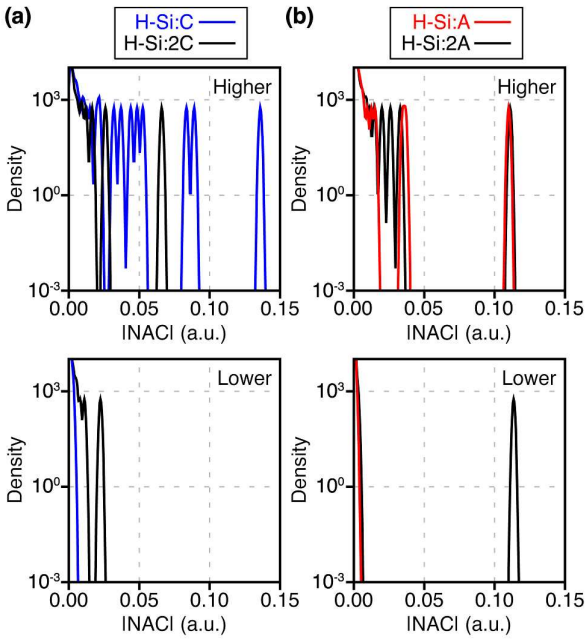

Figure 4. Probability/distribution of nonadiabatic coupling (NAC) as a function of NAC magnitude (in a.u.) between the hot electron state and higher-lying/lower-lying semiconductor states for the (a) Cyanidin and (b) Alizarin cases. Y-axis is shown in log scale. Bin size of 5×10^{-4} was used for the Gaussian broadening where $\sigma^2=5\times10^{-7}$.

Comparing the two different surface coverages, one might have naively assumed that increased surface coverage would enhance the HET process from semiconductor to the adsorbed molecule simply because the number of the hot electron states increases as well. However, the results show otherwise because inter-molecular interaction changes the nature of hot electron states (Figure 3a). As can be seen in Figure 3b, the hot electron states for the high-coverage cases are not the same as the hot electron states for the low-coverage cases. The hot electron states do not remain localized on individual molecules when inter-molecular interactions are present (i.e. when the surface coverage is increased), and the electronic states become highly delocalized. In the case of Alizarin, the hot electron state simply becomes more delocalized over both molecules because of hybridization in the high-coverage case (Figure 3b). However, for the Cyanidin case, the hot electron state is not simply the delocalized state due to inter-molecular interactions, but some other molecular states are more efficient in accepting the hot electron for the high coverage case. Our analysis shows that the delocalization in this case is not simply due to the inter-molecular interaction but it strongly has to do with the interaction of the highly-polar Cyanidin molecules with the semiconductor surface. Without the surface, the hot electron states remain localized on individual molecule, but the surface causes the states to not only delocalize but to also change its spatial character (see Figure S4 in the Supporting Information for details).

To understand this result of the first-principles dynamics simulations, we herein examine nonadiabatic couplings (NACs) since they have previously been found to play a key role in determining HET efficiency.[29,70] Figure 4 shows the probability distribution of the magnitude of the NACs between the hot electron state and higher-lying/lower-lying semiconductor states (i.e. semiconductor states energetically higher/lower than the hot electron state). For the Cyanidin case (**H-Si:C** vs. **H-Si:2C**) as shown in Figure 4a, the low-coverage interface exhibits larger magnitudes for the NACs between the hot electron state and higher-lying semiconductor states than the high-coverage interface. The hot electron is therefore much more likely to transfer into the molecule at the low-coverage interface. NAC magnitudes with lower-lying semiconductor states are significantly smaller at the low-coverage **H-Si:C** interface, making the hot electron state quite effective in retaining the excited electron within the adsorbed molecule for an extended time. For the Alizarin case (**H-Si:A** vs. **H-Si:2A**) as shown in Figure 4b, the low- and high-coverage interfaces exhibit similar NAC magnitudes, including the presence of a well-defined peak for the NACs of ~0.11 a.u.. This gives rise to the similar HET rate as can be seen in Figure 3a; the rate of the initial increase in the probability for **H-Si:A** and **H-Si:2A** are the same (i.e. two red lines are on top of each other). At the same time, for the NACs between the hot electron state and lower-lying semiconductor states, only the high-coverage case of **H-Si:2A** exhibits large NACs of ~0.12 a.u. but not **H-Si:A** (Figure 4b). This yields a rapid hot electron transfer from the adsorbed molecule back to the semiconductor at the **H-Si:2A** interface. Consequently, the hot electron residence time within the adsorbate is much shorter for the **H-Si:2A** interface than for the **H-Si:A** interface as summarized in Table 1. These characteristics in the NACs between the semiconductor and the molecule lead to the significant difference between the low and high-coverage interfaces in terms of the HET efficiency.

Another point of comparison in the simulations is the differences between the Cyanidin and Alizarin molecules; the **H-Si:A** interface shows much larger HET probability than the **H-Si:C** interface. This can be explained by the difference in the NACs between the hot electron state and the lower-lying semiconductor states. Larger NACs for the **H-Si:C** interface (see Figure S7 in the Supporting Information) allow faster return of the excited electron from the adsorbed molecule back to the semiconductor, inhibiting the probability build-up for the hot electron state localized on the molecule. The electronic energy level alignment is another ingredient that is also responsible for the quantum dynamics. To examine if the significant HET probability for the **H-Si:A** interface case could also be due to the fact that its hot electron state is energetically close to the initial state the hot electron occupies in the semiconductor, we performed another simulation for the **H-Si:A** interface with the hot electron state that is artificially shifted away to be at the same energy as the **H-Si:C** case. This artificially-constructed **H-Si:A** simulation yields even higher HET probability (see Figure S8 in the Supporting Information), showing that energetic proximity of the hot electron state to the initial semiconductor state is not the reason for the significant HET probability observed at the **H-Si:A** interface.

Conclusions

In conclusion, we discussed how the surface coverage and molecular adsorbate species influence the hot electron transfer (HET) at semiconductor-molecule interfaces using first-principles electron dynamics simulations. Our work shows that the increased surface coverage does not necessarily enhance the HET probability because of inter-molecular interactions. The accepting molecular states for the hot electron can be delocalized among the adsorbed molecules at the semiconductor surface, and the nonadiabatic couplings can be altered as a result. In fact, for both the Alizarin and Cyanidin molecules we considered here, the HET probability from semiconductor to the adsorbed molecule is significantly suppressed when the surface coverage is increased. The nature of adsorbed molecules itself was found to affect the HET significantly. Fundamental reason for these observations can be traced back to the decisive role nonadiabatic couplings play in controlling the HET across the semiconductor surface and the adsorbed molecule. Developing a “design principle” at a molecular level for enhancing the HET process at semiconductor-molecule interfaces remains a great challenge, and controlling nonadiabatic couplings must be part of such a design principle in addition to the electron energy alignment as is often discussed already.

Conflicts of interest

There are no conflicts to declare.

Acknowledgements

This work was supported solely by the UNC Energy Frontier Research Center (EFRC) “Center for Solar Fuels”, an EFRC funded by the U.S. Department of Energy, Office of Science, Office of Basis Energy Sciences, under Award DE-SC0001011. We thank the National Energy Research Scientific Computing Center, which is supported by the U.S. Department of Energy, Office of Science, under Contract No. DE AC02-05CH11231 for computational resources. We are pleased to acknowledge the Department of Chemistry at the University of North Carolina at Chapel Hill, which is celebrating its 200th anniversary, 1818-2018.

References

1 A. Akbari and P. Berini, *Appl. Phys. Lett.*, 2009, 95, 021104.
2 D. Sun, G. Aivazian, A. M. Jones, J. S. Ross, W. Yao, D. Cobden and X. Xu, *Nat. Nanotechnol.*, 2012, 7, 114-118.
3 A. Sobhani, M. W. Knight, Y. Wang, B. Zheng, N. S. King, L. V. Brown, Z. Fang, P. Nordlander and N. J. Halas, *Nat. Commun.*, 2013, 4, 1643.
4 M. L. Brongersma, N. J. Halas and P. Nordlander, *Nat. Nanotechnol.*, 2015, 10, 25-34.

5 H. A. Atwater and A. Polman, *Nat. Mater.*, 2010, 9, 205-213.
6 C. Clavero, *Nat. Photonics*, 2014, 8, 95-103.
7 S. Yu, Y. H. Kim, S. Y. Lee, H. D. Song and J. Yi, *Angew. Chem., Inter. Ed.* 2014, 126, 11385-11389.
8 S. Linic, P. Christopher and D. B. Ingram, *Nat. Mater.*, 2011, 10, 911-921.
9 R. T. Ross and A. J. Nozik, *J. Appl. Phys.*, 1982, 53, 3813-3818.
10 P. Würfel, *Sol. Energy Mater. Sol. Cells*, 1997, 46, 43-52.
11 B. O'Regan and M. Gratzel, *Nature*, 1991, 353, 737-740.
12 M. A. Henderson, J. M. White, H. Uetsuka and H. Onishi, *J. Am. Chem. Soc.*, 2003, 125, 14974-14975.
13 M. Graetzel, R. A. J. Janssen, D. B. Mitzi and E. H. Sargent, *Nature*, 2012, 488, 304-312.
14 O. V. Prezhdo, W. R. Duncan and V. V. Prezhdo, *Acc. Chem. Res.*, 2008, 41, 339-348.
15 O. V. Prezhdo, W. R. Duncan and V. V. Prezhdo, *Prog. Surf. Sci.*, 2009, 84, 30-68.
16 Z. Zhang and J. T. Yates, *Chem. Rev.*, 2012, 112, 5520-5551.
17 A. V. Akimov, A. J. Neukirch and O. V. Prezhdo, *Chem. Rev.*, 2013, 113, 4496-4565.
18 A. Pandey and P. Guyot-Sionnest, *J. Phys. Chem. Lett.*, 2010, 1, 45-47.
19 J. B. Sambur, T. Novet and B. A. Parkinson, *Science*, 2010, 330, 63-66.
20 W. A. Tisdale, K. J. Williams, B. A. Timp, D. J. Norris, E. S. Aydil and X.-Y. Zhu, *Science*, 2010, 328, 1543-1547.
21 W. A. Tisdale and X.-Y. Zhu, *Proc. Natl. Acad. Sci.*, 2011, 108, 965-970.
22 Y. Tian and T. Tatsuma, *J. Am. Chem. Soc.*, 2005, 127, 7632-7637.
23 A. Furube, L. Du, K. Hara, R. Katoh and M. Tachiya, *J. Am. Chem. Soc.*, 2007, 129, 14852-14853.
24 K. Wu, W. E. Rodríguez-Córdoba, Y. Yang and T. Lian, *Nano Lett.*, 2013, 13, 5255-5263.
25 K. Wu, J. Chen, J. R. McBride and T. Lian, *Science*, 2015, 349, 632-635.
26 S. Tan, L. Liu, Y. Dai, J. Ren, J. Zhao and H. Petek, *J. Am. Chem. Soc.*, 2017, 139, 6160-6168.
27 S. G. Abuabara, L. G. C. Rego and V. S. Batista, *J. Am. Chem. Soc.*, 2005, 127, 18234-18242.
28 J. E. Elenewski, J. Y. Cai, W. Jiang and H. Chen, *J. Phys. Chem. C*, 2016, 120, 20579-20587.
29 L. Li and Y. Kanai, *J. Phys. Chem. Lett.*, 2016, 7, 1495-1500.
30 W. R. Duncan, W. M. Stier and O. V. Prezhdo, *J. Am. Chem. Soc.*, 2005, 127, 7941-7951.
31 E. Jakubikova, R. C. Snoeberger III, V. S. Batista, R. L. Martin and E. R. Batista, *J. Phys. Chem. A*, 2009, 113, 12532-12540.
32 R. Long and O. V. Prezhdo, *J. Am. Chem. Soc.*, 2011, 133, 19240-19249.
33 Y. Han, S. Tretiak and D. Kilin, *Mol. Phys.*, 2014, 112, 474-484.
34 G. A. Tritsaris, D. Vinichenko, G. Kolesov, C. M. Friend and E. Kaxiras, *J. Phys. Chem. C*, 2014, 118, 27393-27401.
35 G. Kolesov, D. Vinichenko, G. A. Tritsaris, C. M. Friend and E. Kaxiras, *J. Phys. Chem. Lett.*, 2015, 6, 1624-1627.
36 M. K. L. Man, A. Margiolakis, S. Deckoff-Jones, T. Harada, E. L. Wong, M. B. M. Krishna, J. Madéo, A. Winchester, S. Lei, R. Vajtai, P. M. Ajayan and K. M. Dani, *Nat. Nanotechnol.*, 2017, 12, 36-40.
37 H. Petek, *Nat. Nanotechnol.*, 2017, 12, 3-4.
38 L. Li, J. C. Wong and Y. Kanai, *J. Chem. Theory Comput.*, 2017, 13, 2634-2641.
39 J. C. Tully, *J. Chem. Phys.*, 1990, 93, 1061-1071.
40 S. Hammes-Schiffer and J. C. Tully, *J. Chem. Phys.*, 1994, 101, 4657-4667.
41 P. V. Parandekar and J. C. Tully, *J. Chem. Phys.*, 2005, 122, 094102.
42 M. S. Hybertsen and S. G. Louie, *Phys. Rev. Lett.*, 1985, 55, 1418-1421.
43 M. S. Hybertsen and S. G. Louie, *Phys. Rev. B*, 1986, 34, 5390-5413.
44 G. Onida, L. Reining and A. Rubio, *Rev. Mod. Phys.*, 2002, 74, 601-659.
45 F. Gygi, *IBM J. Res. Dev.*, 2008, 52, 137-144.
46 D. R. Hamann, M. Schlüter and C. Chiang, *Phys. Rev. Lett.*, 1979, 43, 1494-1497.
47 J. P. Perdew, K. Burke and M. Ernzerhof, *Phys. Rev. Lett.*, 1996, 77, 3865-3868.
48 C. Hu, O. Sugino, H. Hirai and Y. Tateyama, *Phys. Rev. A*, 2010, 82, 062508.
49 R. W. Godby and R. J. Needs, *Phys. Rev. Lett.*, 1989, 62, 1169-1172.
50 A. Oschlies, R. W. Godby and R. J. Needs, *Phys. Rev. B*, 1995, 51, 1527-1535.
51 A. Marini, C. Hogan, M. Grüning and D. Varsano, *Comput. Phys. Commun.*, 2009, 180, 1392-1403.
52 G. Paolo, B. Stefano, B. Nicola, C. Matteo, C. Roberto, C. Carlo, C. Davide, L. C. Guido, C. Matteo, D. Ismaila, C. Andrea Dal, G. Stefano de, F. Stefano, F. Guido, G. Ralph, G. Uwe, G. Christos, K. Anton, L. Michele, M.-S. Layla, M. Nicola, M. Francesco, M. Riccardo, P. Stefano, P. Alfredo, P. Lorenzo, S. Carlo, S. Sandro, S. Gabriele, P. S. Ari, S. Alexander, U. Paolo and M. W. Renata, *J. Phys.: Condens. Matter*, 2009, 21, 395502.
53 M. Bernardi, D. Vigil-Fowler, J. Lischner, J. B. Neaton and S. G. Louie, *Phys. Rev. Lett.*, 2014, 112, 257402.
54 M. Barbatti, *Wiley Interdiscip. Rev.: Comput. Mol. Sci.*, 2011, 1, 620-633.
55 J. C. Tully, *J. Chem. Phys.*, 2012, 137, 22A301.
56 F. de Carvalho, M. Bouduban, B. Curchod and I. Tavernelli, *Entropy*, 2014, 16, 62.
57 M. Bernardi, D. Vigil-Fowler, C. S. Ong, J. B. Neaton and S. G. Louie, *Proc. Natl. Acad. Sci. U. S. A.*, 2015, 112, 5291-5296.
58 J. I. Mustafa, M. Bernardi, J. B. Neaton and S. G. Louie, *Phys. Rev. B*, 2016, 94, 155105.
59 V. A. Jhalani, J.-J. Zhou and M. Bernardi, *Nano Lett.*, 2017, 17, 5012-5019.
60 M. Bernardi, *Eur. Phys. J. B*, 2016, 89, 239.
61 R. Huber, J.-E. Moser, M. Grätzel and J. Wachtveitl, *J. Phys. Chem. B*, 2002, 106, 6494-6499.
62 W. Stier, W. R. Duncan and O. V. Prezhdo, *Adv. Mater.*, 2004, 16, 240-244.
63 F. E. Doany, D. Grischkowsky and C. C. Chi, *Appl. Phys. Lett.*, 1987, 50, 460-462.
64 F. E. Doany and D. Grischkowsky, *Appl. Phys. Lett.*, 1988, 52, 36-38.
65 J. R. Goldman and J. A. Prybyla, *Phys. Rev. Lett.*, 1994, 72, 1364-1367.
66 S. Jeong, H. Zacharias and J. Bokor, *Phys. Rev. B*, 1996, 54, R17300-R17303.
67 T. Sjodin, H. Petek and H.-L. Dai, *Phys. Rev. Lett.*, 1998, 81, 5664-5667.
68 T. Ichibayashi and K. Tanimura, *Phys. Rev. Lett.*, 2009, 102, 087403.
69 G. Boschloo and A. Hagfeldt, *Acc. Chem. Res.*, 2009, 42, 1819-1826.

70 E. Cánovas, H. Wang, M. Karakus and M. Bonn, *Chem. Phys.*, 2016, 471, 54-58.

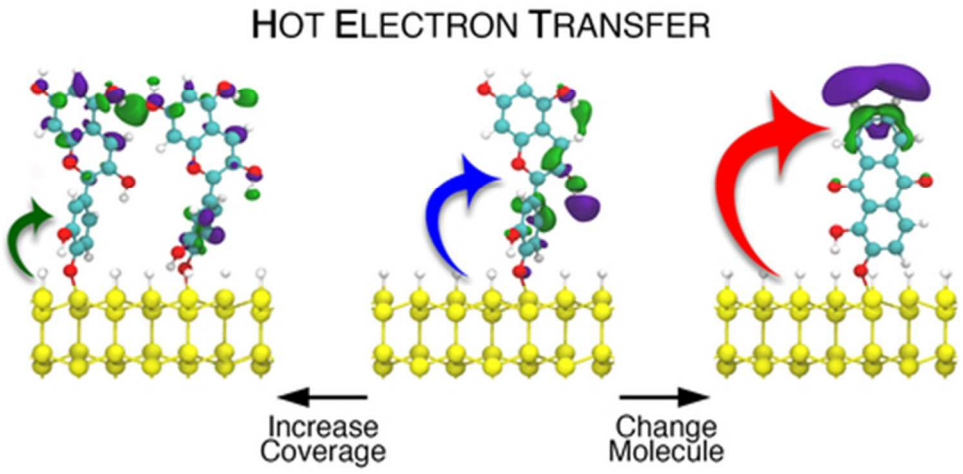

41x20mm (300 x 300 DPI)